Summer 8-12-2016

Limiting Forms of Iterated Circular Convolutions of Planar Polygons

Boyan Kostadinov
CUNY New York City College of Technology

Int. J. Appl. Comp. Math. (Springer) manuscript No.
(will be inserted by the editor)

Limiting Forms of Iterated Circular Convolutions of Planar Polygons

Boyan Kostadinov

Accepted: August, 2016.

Abstract We consider a complex representation of an arbitrary planar polygon $\mathcal{P}$ centered at the origin. Let $\mathcal{P}^{(1)}$ be the normalized polygon obtained from $\mathcal{P}$ by connecting the midpoints of its sides and normalizing the vector of vertex coordinates. We say that $\mathcal{P}^{(1)}$ is a normalized average of $\mathcal{P}$. We identify this averaging process with a special case of a circular convolution. We show that if the normalized convolution is repeated many times, then for a large class of generic (e.g. randomly generated) polygons the vertices of the limiting polygon arrange themselves around an ellipse. There are special classes of polygons, such as the class of star-shaped polygons for which this elliptical limiting behavior does not hold. We show that the star-shaped polygons with zero centroids are closed under circular convolution with normalization. We derive a complete and compact analytical description of the limiting elliptical envelope in the generic case, using discrete Fourier transforms. In the case of generic polygons, one of the key insights of this approach is the realization that the repeated, normalized circular convolution removes all higher harmonic pairs leaving only the principal harmonic pair from the discrete Fourier transform of the original polygon to dominate the Fourier transform of the repeatedly convolved and normalized polygon, thereby controlling the limiting behavior.

Keywords discrete Fourier transform · repeated circular convolution · limiting behavior of convolved and normalized polygons · polygon averaging with normalization · complex representation of an ellipse

Boyan Kostadinov
NYC College of Technology, CUNY
300 Jay St, Brooklyn, NY 11201
E-mail: bkostadinov@citytech.cuny.edu

1 Introduction

Suppose we have an arbitrary planar polygon $\mathcal{P}$ with N vertices. Let $\mathbf{x} = (x_k) \in \mathbb{R}^N$ and $\mathbf{y} = (y_k) \in \mathbb{R}^N$ be the vectors of x and y coordinates that specify the vertices of $\mathcal{P}$, connected in order to form the N-gon.

We consider a simple construction, which starts with one polygon and returns a new polygon whose vertices are the midpoints of the edges of the original one. Thus, we construct a new N-gon $\mathcal{P}^{(1)}$ by averaging the vertices of the old N-gon. We show this averaging process in Figure 1, where we consider a regular pentagon and two steps in the averaging procedure. The original pentagon is blue, the pentagon obtained after one averaging is red, and the pentagon obtained after a second averaging is green.

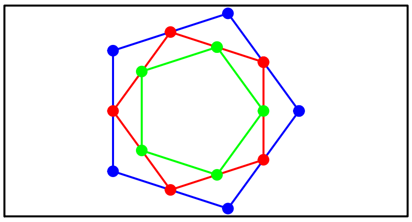

Fig. 1 Two steps in the averaging process for a regular pentagon.

The present study of repeated polygon averaging with normalization was inspired by the paper From Random Polygon to Ellipse: An Eigenanalysis [1, SIAM Review, 2010], where the authors use matrix eigen-analysis to investigate the limiting behavior of randomly generated planar polygons. In our paper, we take a different, yet completely natural, analytical approach from that of [1], and use complex representations of planar polygons and a different normalization procedure. We reformulate the same problem of repeated polygon averaging with normalization, as stated in [1], in terms of iterated, normalized circular convolutions modulo N, thus allowing the tools of Fourier analysis to be used to solve the same problem but in a more straightforward and insightful way, free from any matrix analysis. The main problem is stated in [1, SIAM Review, 2010] as the following Conjecture:

> No matter how random the initial polygon, the edges of the repeatedly convolved and normalized polygon eventually 'uncross', and in the limit the vertices appear to arrange themselves around an ellipse ...

The elliptical limiting behavior is valid for a large class of generic planar polygons (e.g. randomly generated ones) but not all planar polygons. We give an example of a special class of star-shaped polygons for which the elliptical limiting behavior does not hold. For this class of polygons, the iterated, normalized circular convolutions result in a rotated and scaled down copy of the original star-shaped polygon with zero centroid. We also took on the challenge that was expressed at the end of [1] to investigate the higher-dimensional case. After some preliminary computer experiments, we understood how to generalize the planar results to the higher-dimensional case, again using Fourier analysis. We hope to complete and publish soon the results in the higher-dimensional case.

In [1], we find only two general references and no discussion about the long history of this problem that appears to have fascinated many mathematicians since the 19th century. In that regard, we attempt to give a somewhat more complete account of the history of this problem and related ones, to the best of our knowledge. The topic of using Fourier representations of polygons, along with circulant matrices to study the smoothing behavior of iterated averaging transformations of planar and nonplanar polygons, mostly without normalization, has a long history and an extensive literature devoted to it, starting from a paper by Darboux written in 1878 [2], where he solved the problem of polygon averaging without normalization, using a Fourier approach. Jesse Douglas, who won the Fields Medal in 1936 for solving the Plateau problem, studied the geometry of polygons in the complex plane, along with problems of iterated averaging in geometry [3,4], as did E. Kasner in the early 1900s (see the references in [3]). Long after the results by Darboux were forgotten, other researchers rediscovered some of these results. Among them, we mention I. J. Schoenberg in 1950 [5], J. H. Cadwell in 1953 [6], E. R. Berlekamp et al. in 1965 [7], L. Fejes Tóth in 1969 [8,9], P. J. Davis in 1977 [10], R. J. Clarke in 1979 [11]. In particular, in [11], we find another matrix-based study of sequences of polygons, while [7] considers a form of polygon normalization in the planar case, using a Fourier approach, and concludes with comments on repeated averaging of nonplanar polygons without normalization. Many other researchers worked on related problems connecting Fourier analysis with Euclidean geometry, see [12,13,14,15,16,17,18,19,20], and the references therein. We should mention that in [15] Chang and Davis placed the problem of iterative processes in geometry within the context of circulant matrices, while in [12] P. J. Davis placed the Napoleon-Douglas-Neumann theorem within the same context. Circulant matrices can be understood as the matrix representations of circular convolutions - an idea developed in [20] to give a simple description of circulant polygon transformations and their iterates in the context of Napoleon's and the Petr-Douglas-Neumann theorem.

The midpoint averaging is a linear map, which commutes with affine transformations of the plane. There has been much recent progress in the study of somewhat similar but non-linear construction, which commutes with projective transformations and iterates polygons in the setting of projective (rather than affine) geometry. One of these discrete dynamical systems is the *Pentagram Map* that has attracted much attention recently. Another is the *Projective Heat Map*. See R. E. Schwartz's forthcoming research monograph [21]. In the context of multiscale filtering of signals (including digital imaging), introduced by Witkin [22], polygon normalizations appear in affine invariant evolution processes for smoothing planar curves, derived from an affine geometric heat flow (see [19] and the references therein). In [23], the author proposes an algorithm of evolution of a point set on the plane, based on the results from [1], which drives the whole set to a certain regular configuration, and connections to formation control methods are discussed. In [24], the authors consider a problem of controlling a formation of mobile agents, inspired by the results from [1, 23].

We believe it is worthwhile to use the modern language of circular convolutions and discrete Fourier analysis to understand more simply and elegantly various classical problems in geometry. One of the aims of this paper is to shed new light on this beautiful, classical subject by using the modern tools of Fourier analysis, and attract the attention of students and researchers in engineering, physics and other applied fields. The latter is also one of the reasons we decided to have a somewhat leisurely presentation style, given the diverse readership of this journal.

The paper has two parts: the first part investigates the classical case of repeated polygon averaging without normalization applied to planar polygons, and introduces in this context the modern machinery of circular convolutions to understand the limiting behavior of the repeated polygon averaging in terms of the discrete uniform probability distribution, being the limit of repeated circular convolutions of a non-trivial, finite, discrete probability distribution with itself. The second part investigates the more difficult case with polygon normalizations, using again the language of circular convolutions. We show that if the normalized convolution is repeated sufficiently many times, then the vertices of the limiting polygon lie on an ellipse, specified by the principal components of the discrete Fourier transform of the original polygon. We derive a complete and compact analytical description of the limiting elliptical form using the tools of discrete Fourier analysis.

Alongside the analytical investigations, we carry out some computer experiments using the free and open-source software R [25] to generate regular and random planar polygons for our computer explorations and visualizations. For more details on using R for simulation and visualization insights, we refer the interested reader to [26]. We were tempted to shorten the length of the paper by skipping various details and not including many visualizations. However, our goal was to increase the pedagogical value of the article by providing all details and beginning with a short visual gallery of polygon smoothing.

2 A Visual Gallery of Polygon Smoothing

In this short section, we show three visualizations of repeated averaging with normalization applied to random and star-shaped planar polygons.

Example 1 In Figure 2, we generate a random polygon in blue, centered at the origin, and visualize 20 mid-point polygon averagings, with normalization, colored in gray. We also plot the ordered vertices of the final polygon in red. Even at this stage we can see how the averaged polygons get gradually untangled and the elliptic shape of the limiting polygon starts taking form.

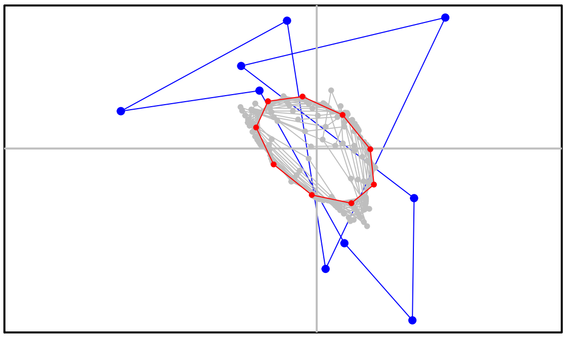

Fig. 2 Untangling of convolved polygons after 20 circular convolutions.

Example 2 In Figure 3, we generate a random polygon centered at the origin and plot in blue the vertices of the limiting polygon after 100 mid-point polygon averagings with normalization.

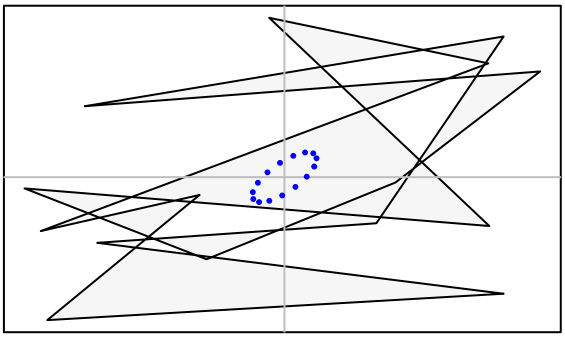

Fig. 3 A random polygon convolved 100 times with normalizations.

In addition to the mid-point averaging process, which is the main interest of our study, we show an example of an arbitrarily weighted averaging, where we take a *weight vector* to be defined as $\mathbf{p} = (p_0, 1 - p_0)$ with $p_0 > 0$.

Example 3 In Figure 4, we plot a 3rd order, star-shaped 11-gon in blue. We then perform 30 steps from the normalized averaging process by plotting the resulting vertices in gray, using the weights $p_0 = 0.98$ and $p_1 = 0.02$. The vertices of the final polygon, after 30 polygon averagings with normalizations, are plotted in red.

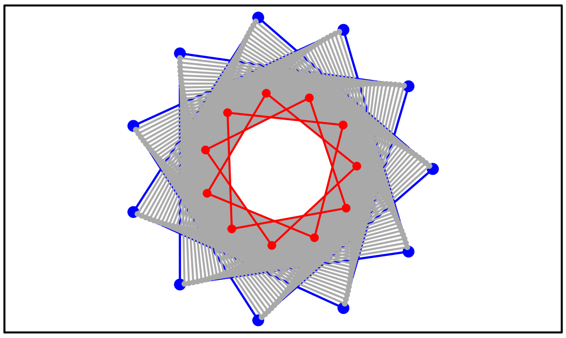

Fig. 4 A 3rd order, star-shaped 11-gon convolved 30 times with $p_0 = 0.98$ and $p_1 = 0.02$.

3 A Complex Representation of a Planar Polygon

Definition 1 (Complex Representation of a Planar Polygon) We define a closed, planar polygon $\mathcal{P} = (\mathcal{P}_k)$, with N vertices, to be a complex vector $\mathbf{z} = (z_k) \in \mathbb{C}^N$, where $z_k = x_k + iy_k$. Here, $x_k = \Re z_k$ and $y_k = \Im z_k$ represent the real coordinates of the k-th vertex $\mathcal{P}_k$ in the plane.

We use the following notation for the vectors of real vertex coordinates: $\mathbf{x} = (x_k)$ and $\mathbf{y} = (y_k)$ in $\mathbb{R}^N$. We index the vertices, starting from 0 index, that is, we let $k = 0, 1, \ldots, N-1$. The closed, planar polygon $\mathcal{P}$ is formed by successively joining the vertices in order, and also by joining the last vertex z_{N-1} with the first one z_0:

$$\mathcal{P} : z_0 \to z_1 \to z_2 \to \cdots \to z_{N-1} \to z_0. \quad (1)$$

The natural periodicity of the vertices of the closed N-gon allows us to extend the finite vector of complex numbers $\mathbf{z} = (z_k)_{k=0}^{N-1}$ into an infinite periodic sequence $(z_k)_{k=0}^{\infty}$ of period N.

Definition 2 We extend the finite complex representation $\mathbf{z} = (z_k)_{k=0}^{N-1}$ of a planar polygon to the infinite, N-periodic sequence $(z_k)_{k=0}^{\infty}$, by defining $z_{k+N} = z_k$ for each index k.

Remark 1 Given this periodicity, we always compute the indices $\bmod N$. This is the reason we take the indices from 0 to $N-1$, rather than 1 to N.

4 A Circular Convolution of Planar Polygons

Let $\mathcal{P}$ be a closed, planar N-gon with a complex representation given by $\mathbf{z} = (z_k)$. We define a weighted averaging of the polygon as follows.

Definition 3 (Weighted Averaging) Let $\mathcal{P}^{(1)}$ be the closed N-gon derived from $\mathcal{P}$ by an averaging procedure, specified by the weight vector $\mathbf{p} = (p_0, p_1)$ such that $p_0 + p_1 = 1$ and $p_0 > 0$, $p_1 > 0$. We define the *weighted averaging of the polygon* in terms of the complex representation $\mathbf{z}^{(1)}$ of $\mathcal{P}^{(1)}$, given by:

$$\mathbf{z}^{(1)} = (p_1 z_{N-1} + p_0 z_0, p_1 z_0 + p_0 z_1, p_1 z_1 + p_0 z_2, \ldots, p_1 z_{N-2} + p_0 z_{N-1}). \quad (2)$$

Remark 2 In Definition 3, the first component of $\mathbf{z}^{(1)}$ represents the averaging of the last and first polygon vertices. The natural periodicity in this N-gon averaging process hints at the idea of using circular convolution modulo N, as a natural framework for this kind of periodic averaging.

Definition 4 (Circular Convolution) Let $\mathbf{p} = (p_0, p_1, \ldots, p_{N-1})$ and $\mathbf{z} = (z_0, \ldots, z_{N-1})$, and consider both sequences as N-periodic. The *circular convolution* of the vector $\mathbf{z} = (z_k)$ with the vector $\mathbf{p} = (p_k)$, denoted by $\mathbf{p} \circledast \mathbf{z}$, is a vector of size N, whose jth component, for $j = 0, \ldots, N-1$, is given by:

$$(\mathbf{p} \circledast \mathbf{z})_j = \sum_{k=0}^{N-1} p_k \, z_{(j-k) \bmod N}, \quad (3)$$

where the indices $(j-k)$ are taken mod N, so that $z_{-1} = z_{N-1}$ etc.

Remark 3 In this paper, we assume that all symbols in bold represent vectors of size N, unless otherwise stated, and whether real or complex should be clear from the context.

The proof of Lemma 1 follows at once from Definition 4:

Lemma 1 *The circular convolution applied to* $\mathbf{p} = (p_0, p_1, 0, \ldots, 0) \in \mathbb{R}^N$ *with* $p_0 + p_1 = 1$ $(p_0, p_1 > 0)$*, and the polygon* $\mathbf{z}$ *gives the polygon weighted averaging, as given in Definition 3:*

$$\mathbf{z}^{(1)} = \mathbf{p} \circledast \mathbf{z} = (p_0 z_0 + p_1 z_{N-1}, p_0 z_1 + p_1 z_0, \ldots, p_0 z_{N-1} + p_1 z_{N-2}). \quad (4)$$

5 Averaging and Normalization Procedure

We construct a new planar N-gon $\mathcal{P}^{(1)}$ by averaging the vertices of the original N-gon. According to Lemma 1, we can identify this averaging process with a particular case of a *circular convolution* $\bmod N$ using a weight vector $\mathbf{p} = (1/2, 1/2, 0, \ldots, 0) \in \mathbb{R}^N$. We are interested in an iterative polygon procedure that involves a coupled polygon vertex averaging and normalization. After each averaging step, we want to normalize the resulting polygon. One approach would be to normalize the real coordinate vectors $\mathbf{x}^{(1)}$ and $\mathbf{y}^{(1)}$ that result from the averaging step, so that they have a unit 2-norm. However, given that we use a complex representation for the planar polygons, we normalize the complex vector $\mathbf{z}^{(1)} \to \mathbf{z}^{(1)}/||\mathbf{z}^{(1)}||$ instead, using the complex 2-norm. We repeat this averaging and normalization process with the goal of understanding analytically the resulting limiting behavior.

6 A Short Review of Discrete Fourier Analysis

We include this short, reference section for completeness, and to avoid confusion that could result from using different normalizations for the discrete Fourier transform, given the diverse readership of this journal, and the fact that people in mathematics, physics and engineering often use slightly different definitions in the context of Fourier analysis. We provide some details about the DFT $\mathcal{F}$, the inverse Fourier transform $\mathcal{F}^{-1}$, the Convolution theorem and Parseval's relation. For the proofs of all theorems in this section, and for more details on discrete Fourier analysis, we refer the reader to [27, 28].

Remark 4 Note that all vectors in this section are considered N-periodic.

6.1 The Discrete Fourier Transform and its Inverse

Definition 5 (Discrete Fourier Transform) Let $\mathbf{Z} = \mathcal{F}[\mathbf{z}] \in \mathbb{C}^N$ be the DFT of the vector $\mathbf{z} = (z_j) \in \mathbb{C}^N$. The kth component Z_k of $\mathbf{Z}$ is given by:

$$Z_k = \mathcal{F}[\mathbf{z}]_k = \sum_{j=0}^{N-1} z_j e^{-i2\pi kj/N}, \quad k = 0, \ldots, N-1. \tag{5}$$

The DFT is invertible.

Theorem 1 (Inverse Fourier Transform) *We get back the original vector $\mathbf{z} = (z_j)$ by applying the inverse discrete Fourier transform $\mathcal{F}^{-1}$ to the vector $\mathbf{Z} = \mathcal{F}[\mathbf{z}]$. The jth component of $\mathcal{F}^{-1}[\mathbf{Z}]$ is exactly equal to z_j:*

$$z_j = \mathcal{F}^{-1}[\mathbf{Z}]_j = \frac{1}{N} \sum_{k=0}^{N-1} Z_k e^{i2\pi jk/N}, \quad j = 0, 1, \ldots, N-1. \tag{6}$$

6.2 The Convolution Theorem

Theorem 2 (The Convolution Theorem) *Let $\mathbf{Z} = (Z_k)$ be the DFT of $\mathbf{z} = (z_k)$ and $\mathbf{W} = (W_k)$ be the DFT of $\mathbf{w} = (w_k)$. We then have the following:*

$$\mathcal{F}[\mathbf{z} \circledast \mathbf{w}] = \mathcal{F}[\mathbf{z}] \circ \mathcal{F}[\mathbf{w}], \tag{7}$$

where the symbol $\circ$ stands for element-wise vector multiplication. We can express (7) component-wise:

$$\mathcal{F}[\mathbf{z} \circledast \mathbf{w}]_k = \mathcal{F}[\mathbf{z}]_k \mathcal{F}[\mathbf{w}]_k = Z_k W_k. \tag{8}$$

6.3 Parseval's Relation

Theorem 3 (Parseval's Relation) *Let* $\mathbf{Z} = (Z_k)$ *be the DFT of* $\mathbf{z} = (z_k)$*. We then have the following equality:*

$$\sum_{k=0}^{N-1} |z_k|^2 = \frac{1}{N} \sum_{k=0}^{N-1} |Z_k|^2. \tag{9}$$

Alternatively, we can express (3) using the complex 2-norm:

$$||\mathbf{z}|| = \frac{1}{\sqrt{N}} ||\mathbf{Z}||. \tag{10}$$

7 Iterated Circular Convolution of Generic Planar Polygons Without Normalization

In this section, we present a novel approach to the classical case of repeated polygon averaging without normalization. Our approach uses the modern language of circular convolutions to understand the limiting behavior of the iterated polygon averaging in terms of the discrete uniform probability distribution, being the limit of the repeated circular convolution of any non-trivial weight vector with itself.

Definition 6 A *non-trivial, weight vector* $\mathbf{p} = (p_0, p_1, \ldots, p_{N-1})$ is defined so that $\sum_k p_k = 1$ and $0 \leq p_k < 1$ for each k, i.e. $\mathbf{p}$ is different from a discrete delta. We can interpret the non-negative weights as probabilities, and the vector $\mathbf{p}$ *as a non-trivial, discrete, finite probability distribution.*

Definition 7 For a given planar polygon $\mathbf{z}$, we define the *centroid* or *center of mass*, denoted by $\langle \mathbf{z} \rangle$, to be the planar point given by the arithmetic mean:

$$\langle \mathbf{z} \rangle = \frac{1}{N} \sum_{k=0}^{N-1} z_k. \tag{11}$$

In this study, we are mostly interested in the specific weight vector $\mathbf{p} = (p_0, p_1, 0, \ldots, 0) \in \mathbb{R}^N$, with $p_0 + p_1 = 1$ and $p_0, p_1 > 0$, as implied by Def. 6.

Lemma 2 *Let* $p = (p_0, p_1, 0, \ldots, 0) \in \mathbb{R}^N$ *be a non-trivial weight vector. The circular convolution* $\bmod N$ *of the polygon* $\mathbf{z}$ *with the weight vector* $\mathbf{p}$ *preserves the centroid of the polygon:*

$$\langle \mathbf{p} \circledast \mathbf{z} \rangle = \langle \mathbf{z} \rangle. \tag{12}$$

Proof The proof follows from Lemma 1, since:

$$\langle \mathbf{p} \circledast \mathbf{z} \rangle = \frac{1}{N} (p_0 z_0 + p_1 z_{N-1} + p_0 z_1 + p_1 z_0 + \cdots + p_0 z_{N-1} + p_1 z_{N-2}) = \langle \mathbf{z} \rangle,$$

where the second equality is obtained after grouping terms involving the same z-components and using that $p_0 + p_1 = 1$. □

Remark 5 Lemma 2 can be generalized for any non-trivial, i.e. different from the discrete delta, weight vector, as given by Definition 6.

Example 4 In Figure 5, a random planar 12-gon is shown after 10, 20 and 50 iterations of circular convolution mod 12, along with the center of mass $\langle \mathbf{z} \rangle$ (the point in red), which remains fixed under circular convolution.

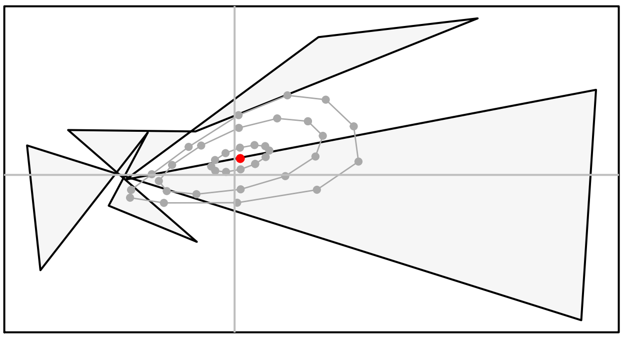

Fig. 5 A random 12-gon after 10, 20 and 50 convolutions and its centroid in red.

The generalization of Lemma 2 for an arbitrary, non-trivial weight vector implies the following:

Corollary 1 *The centroid of any planar polygon* $\mathbf{z}$ *is fixed under repeated circular convolution with any non-trivial weight vector* $\mathbf{p}$*:*

$$\langle \circledast^n \mathbf{p} \circledast \mathbf{z} \rangle = \langle \mathbf{z} \rangle \quad \textit{for any } n \in \mathbb{N}. \tag{13}$$

One of the key results in this section is the following:

Theorem 4 (Central Limit for Circular Convolution) *In the limit of repeated circular convolutions* mod N *of any non-trivial weight vector* $\mathbf{p}$ *with itself, we get the discrete uniform probability distribution:*

$$\lim_{n\to\infty} \circledast^n \mathbf{p} = (1/N, \ldots, 1/N) \in \mathbb{R}^N. \tag{14}$$

Remark 6 Theorem 4 can be interpreted as a form of the *Central Limit Theorem* (CLT) for repeated circular convolutions of finite discrete probability distributions, represented by the weight vector $\mathbf{p}$. The classical CLT for repeated *linear convolutions* of finite, discrete probability distributions, leads to a *Gaussian* shape in the limit.

Proof According to the Convolution Theorem 2, we have the following:

$$\mathcal{F}[\circledast^n \mathbf{p}]_k = \mathcal{F}[\mathbf{p}]_k^n, \text{ for } k = 0, 1, \ldots, N-1, \tag{15}$$

where $\mathbf{P} = \mathcal{F}[\mathbf{p}] \in \mathbb{C}^N$ is the DFT of the weight vector $\mathbf{p} = (p_j)$. According to (5), the kth component is given by:

$$P_k = \mathcal{F}[\mathbf{p}]_k = \sum_{j=0}^{N-1} p_j e^{-i2\pi jk/N}, \quad k = 0, \ldots, N-1, \tag{16}$$

where $p_j \geq 0$ and $\sum p_j = 1$. It follows that $P_0 = \mathcal{F}[\mathbf{p}]_0 = \sum_{j=0}^{N-1} p_j = 1$. For $k \neq 0$, we have:

$$|P_k| = |\mathcal{F}[\mathbf{p}]_k| = \left| \sum_{j=0}^{N-1} p_j e^{-i2\pi jk/N} \right| < \sum_{j=0}^{N-1} \left| p_j e^{-i2\pi jk/N} \right| = \sum_{j=0}^{N-1} p_j = 1. \tag{17}$$

Thus, we have the following limit:

$$\lim_{n\to\infty} \mathcal{F}[\circledast^n \mathbf{p}]_k = \lim_{n\to\infty} \mathcal{F}[\mathbf{p}]_k^n = \lim_{n\to\infty} P_k^n = \delta_{k,0}. \tag{18}$$

Using the continuity of the DFT we have the following:

$$\mathcal{F}[\lim_{n\to\infty} \circledast^n \mathbf{p}]_k = \lim_{n\to\infty} \mathcal{F}[\circledast^n \mathbf{p}]_k = \delta_{k,0}. \tag{19}$$

The component-wise limits imply the following vector identity:

$$\lim_{n\to\infty} \circledast^n \mathbf{p} = \mathcal{F}^{-1}[(1, 0, \ldots, 0)], \tag{20}$$

where $\mathcal{F}^{-1}$ is the inverse DFT, and according to (1), we have:

$$\lim_{n\to\infty} \circledast^n \mathbf{p} = \mathcal{F}^{-1}[(1, 0, \ldots, 0)] = (1/N, \ldots, 1/N) \in \mathbb{R}^N. \tag{21}$$

□

Example 5 In the left panel of Figure 6, we plot a random probability mass function (pmf) $\mathbf{p} \in \mathbb{R}^4$ ($\sum p_k = 1$). In the middle panel, we apply 5 *circular convolutions* to this pmf with itself. Even after 5 convolutions, the limiting distribution appears very close to the discrete uniform distribution $(1/4, \ldots, 1/4)$. In the right panel, we apply 5 *linear convolutions* to the same pmf with itself, and the Gaussian curve starts taking shape.

The next theorem is a modern version of a classical result, first proved by Darboux in 1878 [2], using the language of circular convolutions and the novel observation made in Theorem 4.

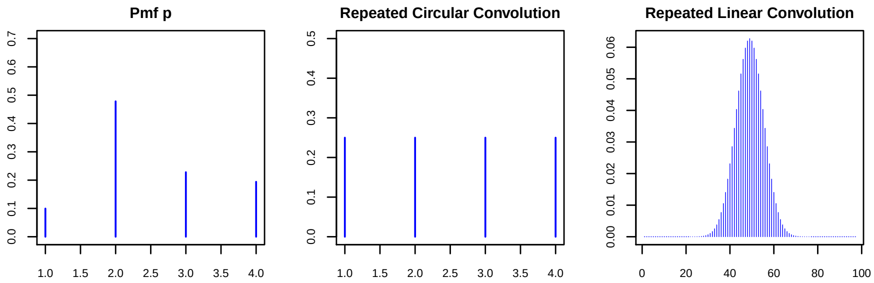

Fig. 6 A pmf and the CLT for repeated circular and linear convolutions of this pmf.

Theorem 5 *In the limit of repeated circular convolutions* mod N *of a generic planar* N*-gon* $\mathbf{z}$*, with any non-trivial weight vector* $\mathbf{p} \in \mathbb{R}^N$*, the polygon collapses to its centroid* $\langle \mathbf{z} \rangle$*. More precisely, we have the following vector-valued limit (computed component-wise) for the sequence of convolved* N*-gons:*

$$\lim_{n\to\infty} \circledast^n \mathbf{p} \circledast \mathbf{z} = (\langle \mathbf{z} \rangle, \ldots, \langle \mathbf{z} \rangle) \in \mathbb{C}^N. \tag{22}$$

Proof According to Theorem 4, we just need to show that circular convolution with the discrete uniform probability distribution results in a vector of N copies of the centroid of $\mathbf{z}$:

$$\left(\frac{1}{N}, \ldots, \frac{1}{N}\right) \circledast (z_0, z_1, \ldots, z_{N-1}) = (\langle \mathbf{z} \rangle, \ldots, \langle \mathbf{z} \rangle) \in \mathbb{C}^N. \tag{23}$$

Verifying this identity is a simple application of Definition 4, and we leave it as an exercise for the reader. □

8 Iterated Normalized Circular Convolutions

In this section, we consider iterated, normalized circular convolutions of a generic, planar N-gon $\mathbf{z}$ with a weight vector $\mathbf{p} = (1/2, 1/2, 0, \ldots, 0) \in \mathbb{R}^N$. We start with a generic, e.g. randomly generated, planar polygon $\mathbf{z}$ centered at the origin, that is, having a zero centroid $\langle \mathbf{z} \rangle = 0$. Each iteration step, in the algorithm of iterated, normalized circular convolutions, consists of two procedures:

1. Perform a circular convolution of $\mathbf{z}$ with the weight vector $\mathbf{p}$ to obtain the averaged polygon $\mathbf{w}^{(1)}$.
2. Normalize the resulting polygon $\mathbf{w}^{(1)}$ into $\mathbf{z}^{(1)}$ to have a unit 2-norm.

Remark 7 According to Lemma 2, the centroid of the convolved polygon is fixed under circular convolution with a weight vector, thus all convolved polygons remain centered at the origin.

The next iteration step repeats procedures 1. and 2. above. More precisely, we have the following sequence of transformations:

$$\text{Iteration Step 1: } \mathbf{w}^{(1)} = \mathbf{p} \circledast \mathbf{z} \to \mathbf{z}^{(1)} = \frac{\mathbf{w}^{(1)}}{||\mathbf{w}^{(1)}||} = \frac{\mathbf{p} \circledast \mathbf{z}}{||\mathbf{p} \circledast \mathbf{z}||}. \quad (24)$$

$$\text{Iteration Step 2: } \mathbf{z}^{(2)} = \frac{\mathbf{p} \circledast \mathbf{z}^{(1)}}{||\mathbf{p} \circledast \mathbf{z}^{(1)}||} = \frac{\circledast^2 \mathbf{p} \circledast \mathbf{z}}{|| \circledast^2 \mathbf{p} \circledast \mathbf{z}||}, \quad (25)$$

where the second equality in Iteration Step 2 follows by linearity of convolution:

$$||\mathbf{p} \circledast \mathbf{z}^{(1)}|| = ||\mathbf{p} \circledast \left(\frac{\mathbf{p} \circledast \mathbf{z}}{||\mathbf{p} \circledast \mathbf{z}||} \right)|| = \frac{|| \circledast^2 \mathbf{p} \circledast \mathbf{z}||}{||\mathbf{p} \circledast \mathbf{z}||}. \quad (26)$$

The nth step in this iteration procedure gives:

$$\text{Iteration Step } n\text{: } \mathbf{w}^{(n)} = \circledast^n \mathbf{p} \circledast \mathbf{z} \to \mathbf{z}^{(n)} = \frac{\circledast^n \mathbf{p} \circledast \mathbf{z}}{|| \circledast^n \mathbf{p} \circledast \mathbf{z}||} = \frac{\mathbf{w}^{(n)}}{||\mathbf{w}^{(n)}||}. \quad (27)$$

Remark 8 The linearity of convolution implies that the iterated sequence of alternating convolution and normalization for finite sequences is equivalent to convolving without normalizing at each step, but rather normalizing at the final step only. In that regard, the n-fold convolution before the final normalization is $\mathbf{w}^{(n)} = \circledast^n \mathbf{p} \circledast \mathbf{z}$. For the final, normalized polygon $||\mathbf{z}^{(n)}|| = 1, \langle \mathbf{z}^{(n)} \rangle = 0$. The algorithm of iterated, normalized circular convolutions gives a sequence of polygons $\mathbf{z}$, $\mathbf{z}^{(1)}$,$\mathbf{z}^{(2)}$,. . .,$\mathbf{z}^{(n)}$, whose limiting behavior we now investigate.

First, we want to investigate the structure of the n-fold circular convolution of the original polygon, without normalization.

Definition 8 Let $\mathbf{w}^{(n)} = \circledast^n \mathbf{p} \circledast \mathbf{z}$ be the nth fold circular convolution without normalization. The nth fold normalized polygon is then $\mathbf{z}^{(n)} = \mathbf{w}^{(n)}/||\mathbf{w}^{(n)}||$.

Theorem 6 *Let $\mathbf{W}^{(n)} = (W_k^{(n)})$ be the DFT of $\mathbf{w}^{(n)}$, and $\mathbf{Z} = (Z_k)$ be the DFT of the initial, generic polygon $\mathbf{z}$. For each $k = 0, 1, \ldots, N-1$, we have:*

$$W_k^{(n)} = \mathcal{F}[\mathbf{p}]_k^n Z_k = e^{-i\pi kn/N} \cos^n(\pi k/N) Z_k. \quad (28)$$

Proof The Convolution Theorem (2) implies:

$$\mathbf{W}^{(n)} = \mathcal{F}[\mathbf{w}^{(n)}] = \mathcal{F}[\circledast^n \mathbf{p} \circledast \mathbf{z}] = \mathcal{F}[\circledast^n \mathbf{p}] \circ \mathcal{F}[\mathbf{z}], \quad (29)$$

where the $\circ$ operator is the element-wise multiplication of vectors. We can write this vector equation component-wise:

$$W_k^{(n)} = \mathcal{F}[\circledast^n \mathbf{p}]_k Z_k, \ \ k = 0, 1, 2, \ldots, N-1, \quad (30)$$

where $Z_k = \mathcal{F}[\mathbf{z}]_k$. Applying the Convolution Theorem 2 again, gives:

$$\mathcal{F}[\circledast^n \mathbf{p}] = \mathcal{F}[\mathbf{p}] \circ \cdots \circ \mathcal{F}[\mathbf{p}] = \circ^n \mathcal{F}[\mathbf{p}], \tag{31}$$

where $\circ^n$ represents an element-wise multiplication applied n times. This vector equation, written component-wise, is equivalent to:

$$\mathcal{F}[\circledast^n \mathbf{p}]_k = \mathcal{F}[\mathbf{p}]_k^n. \tag{32}$$

The kth component of the DFT of $\mathbf{p} = (0.5, 0.5, 0, \dots, 0)$, is given by:

$$\mathcal{F}[\mathbf{p}]_k = \sum_{j=0}^{N-1} p_j\, e^{-i2\pi kj/N} = \frac{1}{2}(1 + e^{-i2\pi k/N}) = e^{-i\pi k/N} \cos(\pi k/N), \tag{33}$$

where we used that $\cos(\pi k/N) = \frac{1}{2}(e^{i\pi k/N} + e^{-i\pi k/N})$. Using (30), (32) and (33), we complete the proof:

$$W_k^{(n)} = \mathcal{F}[\mathbf{p}]_k^n Z_k = e^{-i\pi kn/N} \cos^n(\pi k/N) Z_k. \tag{34}$$

□

Theorem 7 *The kth component of the DFT $\mathbf{Z}^{(n)} = (Z_k^{(n)})$ of the normalized sequence of convolved planar polygons $\mathbf{z}^{(n)}$ is given by:*

$$Z_k^{(n)} = \sqrt{N} \frac{e^{-\frac{i\pi kn}{N}} \cos^n\left(\frac{\pi k}{N}\right) Z_k}{\sqrt{\sum_{k=1}^{N-1} |\cos\left(\frac{\pi k}{N}\right)|^{2n} |Z_k|^2}}. \tag{35}$$

Proof

$$\mathcal{F}[\mathbf{z}^{(n)}] = \mathcal{F}\left[\frac{\mathbf{w}^{(n)}}{||\mathbf{w}^{(n)}||}\right] = \frac{\mathcal{F}[\mathbf{w}^{(n)}]}{||\mathbf{w}^{(n)}||}, \tag{36}$$

where in the second equality we used the linearity of the DFT. Parseval's relation (3), gives us a link between the 2-norms of a vector and its DFT:

$$||\mathbf{w}^{(n)}|| = \frac{1}{\sqrt{N}} ||\mathcal{F}[\mathbf{w}^{(n)}]||. \tag{37}$$

From (37) and (36) we have the following:

$$\mathbf{Z}^{(n)} = \mathcal{F}[\mathbf{z}^{(n)}] = \frac{\mathcal{F}[\mathbf{w}^{(n)}]}{||\mathbf{w}^{(n)}||} = \sqrt{N} \frac{\mathcal{F}[\mathbf{w}^{(n)}]}{||\mathcal{F}[\mathbf{w}^{(n)}]||}. \tag{38}$$

We can express this vector equation element-wise:

$$Z_k^{(n)} = \sqrt{N} \frac{\mathcal{F}[\mathbf{w}^{(n)}]_k}{||\mathcal{F}[\mathbf{w}^{(n)}]||} = \sqrt{N} \frac{W_k^{(n)}}{||\mathbf{W}^{(n)}||}, \tag{39}$$

where the complex 2-norm is given by:

$$||\mathbf{W}^{(n)}|| = \sqrt{\sum_{k=0}^{N-1} |W_k^{(n)}|^2} = \sqrt{\sum_{k=1}^{N-1} |W_k^{(n)}|^2}. \tag{40}$$

In the second equality above, we shifted the starting index from $k = 0$ to $k = 1$ since the centroid is fixed at the origin under circular convolutions, which implies that $W_0^{(n)} = 0$ for each iteration n. From (30), (39) and (40), the kth component ($k = 0, 1, \ldots, N-1$) of the DFT of the normalized polygon after n circular convolutions is given by the expression:

$$Z_k^{(n)} = \sqrt{N} \frac{e^{-\frac{i\pi kn}{N}} \cos^n\left(\frac{\pi k}{N}\right) Z_k}{\sqrt{\sum_{k=1}^{N-1} |\cos\left(\frac{\pi k}{N}\right)|^{2n} |Z_k|^2}}. \tag{41}$$

□

Remark 9 Since the original polygon has a zero centroid, we have that $Z_0 = 0$, hence $Z_0^{(n)} = 0$ for each iteration n.

Theorem 8 (DFT of Normalized, n-fold Convolved N-gon) *The DFT of the normalized N-gon after n circular convolutions* $\bmod N$ *of the weight vector* $\mathbf{p}$ *with the original N-gon* $\mathbf{z}$ *is given by:*

$$\mathbf{Z}^{(n)} = \left(0, \sqrt{N}\, Z_1 \frac{e^{-i\pi n/N}}{M_n}, \mathcal{O}(\alpha^n), \ldots, \mathcal{O}(\alpha^n), \sqrt{N}\, Z_{N-1} \frac{e^{i\pi n/N}}{M_n}\right), \tag{42}$$

where M_n is defined in (54), and α is defined in (48).

Proof The DFT of the normalized polygon after n circular convolutions has the following general structure:

$$\mathbf{Z}^{(n)} = (0, Z_1^{(n)}, \ldots, Z_{N-1}^{(n)}) \in \mathbb{C}^N, \tag{43}$$

where each component $Z_k^{(n)} = \sqrt{N} W_k^{(n)} / ||\mathbf{W}^{(n)}||$. In particular, from (30) we have the following expressions for the principal harmonic pair $(W_1^{(n)}, W_{N-1}^{(n)})$ in the DFT of the nth fold convolved polygon without normalization:

$$W_1^{(n)} = e^{-i\pi n/N} \cos^n(\pi/N)\, Z_1, \tag{44}$$

$$W_{N-1}^{(n)} = e^{-i\pi(N-1)n/N} \cos^n(\pi(N-1)/N)\; Z_{N-1} \tag{45}$$

$$= (-1)^n e^{i\pi n/N} \left(-\cos(\pi/N)\right)^n\; Z_{N-1} \tag{46}$$

$$= e^{i\pi n/N} \cos^n(\pi/N)\; Z_{N-1}. \tag{47}$$

The components $Z_1^{(n)}$ and $Z_{N-1}^{(n)}$ of the DFT $\mathbf{Z}^{(n)}$ dominate the other components, which tend to 0 very fast as the number of convolutions n gets large. To see this, we look into the structure of the components:

$$
\begin{aligned}
Z_1^{(n)} &= \frac{\sqrt{N}e^{-i\pi n/N}\cos^n(\pi/N)\,Z_1}{\sqrt{\cos^{2n}(\pi/N)\,(|Z_1|^2+|Z_{N-1}|^2)+\cos^{2n}(2\pi/N)\,|Z_2|^2+\cdots}} \\
&= \frac{\sqrt{N}e^{-i\pi n/N}Z_1}{\sqrt{|Z_1|^2+|Z_{N-1}|^2+\mathcal{O}(\alpha^{2n})}},
\end{aligned}
$$

where we used that $\cos(\pi/N) > 0$ for $N \geq 3$, and all remaining terms in the denominator for $k \neq \{1, N-1\}$ are of order $\mathcal{O}(\alpha^{2n})$ as $\lim_{n\to\infty} \alpha^{2n} = 0$ for $|\alpha| < 1$, and α is defined to be:

$$
\alpha = \frac{\cos(2\pi/N)}{\cos(\pi/N)} \in [0,1) \text{ for } N \geq 4. \tag{48}
$$

Similarly, we have:

$$
Z_{N-1}^{(n)} = \frac{\sqrt{N}e^{i\pi n/N}Z_{N-1}}{\sqrt{|Z_1|^2+|Z_{N-1}|^2+\mathcal{O}(\alpha^{2n})}}. \tag{49}
$$

On the other hand, the $k = 2$ component has the following structure:

$$
\begin{aligned}
Z_2^{(n)} &= \frac{\sqrt{N}e^{-i\pi 2n/N}\cos^n(2\pi/N)Z_2}{\cos^n(\pi/N)\sqrt{|Z_1|^2+|Z_{N-1}|^2+\mathcal{O}(\alpha^{2n})}} \qquad (50)\\
&= \frac{\alpha^n\sqrt{N}e^{-i\pi 2n/N}Z_2}{\sqrt{|Z_1|^2+|Z_{N-1}|^2+\mathcal{O}(\alpha^{2n})}} \qquad (51)\\
&= \mathcal{O}(\alpha^n). \qquad (52)
\end{aligned}
$$

More generally, all higher harmonics in the DFT of $\mathbf{Z}^{(n)}$ have similar structure for $k = 2, 3, \ldots, N-2$:

$$
|Z_k^{(n)}| = \frac{\sqrt{N}|\cos(k\pi/N)|^n\,|Z_k|}{|\cos(\pi/N)|^n\,\sqrt{|Z_1|^2+|Z_{N-1}|^2+\mathcal{O}(\alpha^{2n})}} = \mathcal{O}(\alpha^n). \tag{53}
$$

We make the following definitions:

$$
M_n = \sqrt{|Z_1|^2+|Z_{N-1}|^2+\mathcal{O}(\alpha^{2n})} \text{ and } M = \sqrt{|Z_1|^2+|Z_{N-1}|^2}, \tag{54}
$$

where $\lim_{n\to\infty} M_n = M$, and we have the following vector representation of the DFT of the normalized polygon after n circular convolutions:

$$
\mathbf{Z}^{(n)} = \left(0, \sqrt{N}\,Z_1\,\frac{e^{-i\pi n/N}}{M_n}, \mathcal{O}(\alpha^n), \ldots, \mathcal{O}(\alpha^n), \sqrt{N}\,Z_{N-1}\,\frac{e^{i\pi n/N}}{M_n}\right). \tag{55}
$$

□

Next, we prove one of the main results of this study, valid for a large class of generic, planar polygons (but not all polygons).

Theorem 9 *Repeatedly applying a normalized, circular convolution to a random planar N-gon with zero centroid, results in a limiting polygon inscribed in the ellipse $z(t)$ given by the complex representation:*

$$z(t) = a_1\, e^{i2\pi t} + a_2\, e^{-i2\pi t}, \tag{56}$$

where $a_1 = \frac{Z_1}{\sqrt{N}M}$, $a_2 = \frac{Z_{N-1}}{\sqrt{N}M}$, and $M = \sqrt{|Z_1|^2 + |Z_{N-1}|^2}$. As before, (Z_1, Z_{N-1}) is the principal harmonic pair in the DFT of the original polygon $\mathbf{z}$. The limiting ellipse (56) is inclined at an angle $(Arg(Z_1) + Arg(Z_{N-1}))/2$ relative to the positive real axis. The lengths a and b of the major and minor semi-axis, and the foci distance c from the origin, are given by:

$$a = \frac{|Z_1| + |Z_{N-1}|}{\sqrt{N(|Z_1|^2 + |Z_{N-1}|^2)}}, \tag{57}$$

$$b = \frac{||Z_1| - |Z_{N-1}||}{\sqrt{N(|Z_1|^2 + |Z_{N-1}|^2)}}, \tag{58}$$

$$c = 2\sqrt{\frac{|Z_1||Z_{N-1}|}{N(|Z_1|^2 + |Z_{N-1}|^2)}}. \tag{59}$$

Proof We apply the inverse DFT to $\mathbf{Z}^{(n)}$, using Theorem 1, to get back to the polygon $\mathbf{z}^{(n)}$, obtained after n circular convolutions with normalization, whose kth vertex is given by:

$$z_k^{(n)} = \mathcal{F}^{-1}[\mathbf{Z}^{(n)}]_k = \frac{1}{N}\sum_{j=0}^{N-1} Z_j^{(n)} e^{i2\pi jk/N} \tag{60}$$

$$= \frac{Z_1}{\sqrt{N}}\frac{e^{-i\pi n/N}}{M_n}\, e^{i2\pi k/N} + \frac{Z_{N-1}}{\sqrt{N}}\frac{e^{i\pi n/N}}{M_n}\, e^{-i2\pi k/N} + \mathcal{O}(\alpha^n), \tag{61}$$

where we used that $Z_1^{(n)} = \sqrt{N}\, Z_1\, \frac{e^{-i\pi n/N}}{M_n}$ and $Z_{N-1}^{(n)} = \sqrt{N}\, Z_{N-1}\, \frac{e^{i\pi n/N}}{M_n}$. We can rewrite (61) in the following form:

$$z_k^{(n)} = a_1^{(n)}\, e^{i2\pi k/N} + a_{N-1}^{(n)}\, e^{-i2\pi k/N} + \mathcal{O}(\alpha^n), \tag{62}$$

where we make the following definitions:

$$a_1^{(n)} = \frac{Z_1}{\sqrt{N}}\frac{e^{-i\pi n/N}}{M_n} \text{ and } a_{N-1}^{(n)} = \frac{Z_{N-1}}{\sqrt{N}}\frac{e^{i\pi n/N}}{M_n}. \tag{63}$$

Thus, all vertices of the polygon $\mathbf{z}^{(n)} = (z_k^{(n)})$, obtained after n circular convolutions, lie on the curve given by the complex equation:

$$z_n(t) = a_1^{(n)}\, e^{i2\pi t} + a_{N-1}^{(n)}\, e^{-i2\pi t} + \mathcal{O}(\alpha^n), \tag{64}$$

where the polygon vertices $z_k^{(n)} = z_n(t_k)$ for $t_k = k/N$, $k = 0, 1, \ldots, N-1$. As a function of the number of convolutions n, (62) results in at most $2N$ different limiting forms, thanks to the phase factors $e^{\mp i\pi n/N}$. Thus, $z_n(t)$ is periodic in n with period $2N$. After a large number n of convolutions, the error term $\mathcal{O}(\alpha^n)$ is negligible and the continuous limiting form is given by the curve:

$$z(t) = a_1\, e^{i2\pi t} + a_2\, e^{-i2\pi t}, \tag{65}$$

where $a_1 = \frac{Z_1}{\sqrt{NM}}$, and $a_2 = \frac{Z_{N-1}}{\sqrt{NM}}$. Note that the phase factors $e^{\mp i\pi n/N}$ are absorbed by $e^{\pm i2\pi k/N}$.

The curve $z(t)$ in (65) is actually an ellipse given in a complex form. Essentially, the ellipse is built by the vector sum of the rotated planar vectors a_1 and a_2, given as complex numbers, where the phase factor $e^{i2\pi t}$ rotates a_1 counter-clockwise, and $e^{-i2\pi t}$ rotates a_2 clock-wise, and as t increases from 0 to 1, the resulting vector sum describes a complete ellipse. The parameters of the ellipse are given in terms of the complex numbers a_1 and a_2. Let a_1 and a_2 be given in their polar form:

$$a_1 = |a_1|e^{i\theta_1} \text{ and } a_2 = |a_2|e^{i\theta_2}. \tag{66}$$

For $t_1 = (\theta_2 - \theta_1)/4\pi$ the vectors a_1 and a_2 get both rotated onto the line passing through 0 that makes an angle of $(\theta_1 + \theta_2)/2$ with the positive x-axis, and the two vectors, being in phase, point in the same direction:

$$z(t_1) = (|a_1| + |a_2|)e^{i(\theta_1+\theta_2)/2}. \tag{67}$$

Thus, $a = |a_1| + |a_2|$ is the maximum modulus of $z(t)$, and it is therefore the length of the major semi-axis of the ellipse, which forms an angle $\phi = (\theta_1+\theta_2)/2$ with the positive real axis. Note that $\phi = (Arg(Z_1)+Arg(Z_{N-1}))/2$. Similarly, at $t_2 = (\theta_2 - \theta_1 + \pi)/4\pi$:

$$z(t_2) = (|a_1| - |a_2|)e^{i(\theta_1+\theta_2+\pi)/2}, \tag{68}$$

and the two vectors now point in opposite directions and lie on the minor axis, perpendicular to the major axis (since their arguments differ by $\pi/2$). Thus, $b = ||a_1| - |a_2||$ is the length of the minor semi-axis of the ellipse. The foci lie on the major axis at a distance c from the center of the ellipse. This ellipse is centered at zero since the center is the intersection of the major and minor axes, and they intersect at 0. Since $c^2 = a^2 - b^2 = 4|a_1 a_2|$, we have $c = 2\sqrt{|a_1 a_2|}$. Thus, for the limiting ellipse, we get the expressions for the lengths a and b of the major and minor semi-axis, as well as the foci distance c, as given in (57), (58) and (59). □

Remark 10 If it happens for $|Z_1|$ and $|Z_{N-1}|$ that either one or the other (but not both) is zero, then $z(t)$ is a circle centered at zero of radius $1/\sqrt{N}$. We have a proper ellipse if $|Z_1| \neq |Z_{N-1}|$ and none of the moduli is zero. If $|Z_1| = |Z_{N-1}|$, the minor axis collapses and as a result the ellipse degenerates to the major axis. If $|Z_1| = |Z_{N-1}| = 0$, then the higher harmonic pair Z_2 and Z_{N-2} become the dominant terms in the limiting form, which can be analyzed in a similar way.

Example 6 In Figure 7, we plot the ellipse for a random choice of the vectors a_1 and a_2 controlling its complex representation, as given by (56).

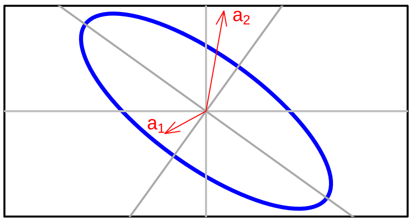

Fig. 7 The ellipse based on its complex representation, for a random choice of a_1 and a_2.

Example 7 In Figure 8, we generate a random polygon with $N = 15$ vertices, with zero centroid. We then perform $n = 100$ normalized circular convolutions on this polygon using the mid-point averaging weight vector $\mathbf{p}$. The resulting 100-fold convolved and normalized polygon is represented by the blue dots. The smaller red dots are computed by the analytical expression that we derived in (62), and the limiting elliptical form $z(t)$, given by (56), is also plotted in red.

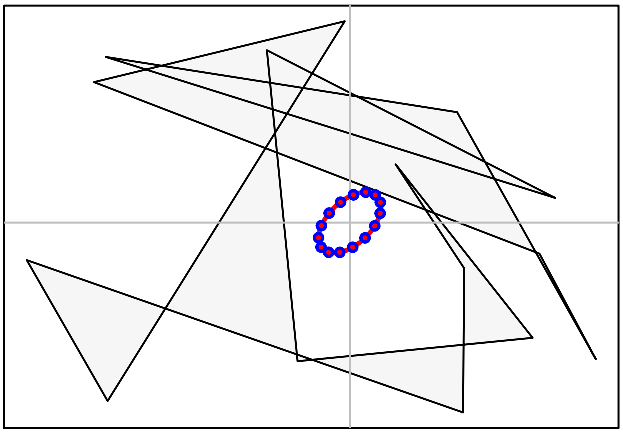

Fig. 8 A random 15-gon with zero centroid, after 100 normalized convolutions.

9 Repeated Circular Convolutions of Star-Shaped Polygons

The elliptical limiting behavior is valid for a large class of generic planar polygons (e.g. randomly generated ones) but not all planar polygons. We now give an example of a special class of star-shaped polygons for which the elliptical limiting behavior does not hold. For this class of polygons, the iterated, normalized circular convolutions result in a rotated and scaled down copy of the original star-shaped polygon.

Definition 9 We define the regular, mth order, *star-shaped polygon* with N vertices, to be given by its complex representation $\mathbf{z} = (z_k)$:

$$z_k = e^{i2\pi mk/N}, \text{ for } m < \lfloor N/2 \rfloor, \tag{69}$$

where $\lfloor N/2 \rfloor$ stands for the integer part, and $k = 0, 1, \ldots, N-1$.

Theorem 10 *The polygon* $\mathbf{z}^{(n)}$*, resulting from* n *circular convolutions with normalization of the regular,* m*th order, star-shaped* N*-gon* $\mathbf{z}$ *is given by:*

$$\mathbf{z}^{(n)} = \frac{e^{-i\pi mn/N}}{\sqrt{N}}\,\mathbf{z}. \tag{70}$$

Proof Let $\mathbf{Z} = (Z_j) = \mathcal{F}[\mathbf{z}]$ be the DFT of the initial polygon $\mathbf{z}$. Component-wise, we have:

$$Z_j = \sum_{k=0}^{N-1} z_k e^{-i2\pi jk/N} = \sum_{k=0}^{N-1} e^{i2\pi k(m-j)/N} = N\delta_{j,m} = \begin{cases} N & \text{if } m = j \\ 0 & \text{if } m \neq j \end{cases} \tag{71}$$

where $\delta_{j,m}$ is the Kronecker delta. Let $\mathbf{W}^{(n)} = (W_k^{(n)})$ be the DFT of the polygon obtained after n circular convolutions, without any normalization, that is $\mathbf{W}^{(n)} = \mathcal{F}[\circledast^n \mathbf{p} \circledast \mathbf{z}]$. Component-wise, by the Convolution theorem:

$$W_k^{(n)} = \mathcal{F}[\circledast^n \mathbf{p}]_k Z_k = \mathcal{F}[\mathbf{p}]_k^n Z_k = e^{-i\pi kn/N}\cos^n(\pi k/N) N\delta_{k,m}. \tag{72}$$

Let $\mathbf{z}^{(n)} = \frac{\circledast^n \mathbf{p} \circledast \mathbf{z}}{||\circledast^n \mathbf{p} \circledast \mathbf{z}||}$ be the complex representation of the normalized polygon after n circular convolutions; its DFT $\mathbf{Z}^{(n)} = (Z_k^{(n)})$ is given by:

$$\mathbf{Z}^{(n)} = \mathcal{F}[\mathbf{z}^{(n)}] = \mathcal{F}\left[\frac{\circledast^n \mathbf{p} \circledast \mathbf{z}}{||\circledast^n \mathbf{p} \circledast \mathbf{z}||}\right] = \sqrt{N}\frac{\mathcal{F}[\circledast^n \mathbf{p} \circledast \mathbf{z}]}{||\mathcal{F}[\circledast^n \mathbf{p} \circledast \mathbf{z}]||} = \frac{\sqrt{N}\mathbf{W}^{(n)}}{||\mathbf{W}^{(n)}||}, \tag{73}$$

where the second equality follows from Parseval's relation between the complex 2-norms of a vector and its DFT. From (72) we can compute the 2-norm:

$$||\mathbf{W}^{(n)}|| = \sqrt{|W_k^{(n)}|^2} = \sqrt{\sum_{k=0}^{N-1} \cos^{2n}(\pi k/N) N^2 \delta_{k,m}} \tag{74}$$

$$= \sqrt{\cos^{2n}(\pi m/N) N^2} = N|\cos^n(\pi m/N)|. \tag{75}$$

Thus, from (72), (73) and (75), we have the following result for the DFT of the normalized star-shaped polygon after n circular convolutions:

$$Z_k^{(n)} = \mathcal{F}[\mathbf{z}^{(n)}]_k = \sqrt{N} e^{-i\pi kn/N} \left(\frac{\cos(\pi k/N)}{|\cos(\pi m/N)|} \right)^n \delta_{k,m}, \tag{76}$$

where $m < \lfloor N/2 \rfloor$ so that the denominator does not vanish. Thus, all components of the DFT $\mathbf{Z}^{(n)}$ are zero, except for the mth component:

$$\mathbf{Z}^{(n)} = (0, 0, \ldots, Z_m^{(n)}, 0, \ldots, 0), \tag{77}$$

where $Z_m^{(n)} = \sqrt{N} e^{-i\pi mn/N}$ since the cosine ratio becomes one for $m < N/2$. We get back to the polygon representation $\mathbf{z}^{(n)}$ resulting from n normalized circular convolutions, by applying the inverse DFT:

$$z_k^{(n)} = \mathcal{F}^{-1}[\mathbf{Z}^{(n)}]_k = \frac{1}{N} \sum_{j=0}^{N-1} Z_j^{(n)} e^{i2\pi jk/N} = \frac{1}{N} Z_m^{(n)} e^{i2\pi mk/N} \tag{78}$$

$$= \frac{z_k}{\sqrt{N}} e^{-i\pi mn/N}. \tag{79}$$

where z_k is the kth vertex of the original polygon $\mathbf{z} = (z_k)$. □

Example 8 In Figure 9, we plot the initial 3rd order, star-shaped 10-gon in blue, and the resulting polygon after 5 normalized, circular convolutions in red. We also plot with blue points the final 5-fold convolved and normalized polygon, coded according to the analytical expression obtained for $\mathbf{z}^{(n)}$ in (70), which represents a rotation and scaling of the original star-shaped polygon.

Concluding Remarks

This study investigates an averaging problem of planar polygons in terms of repeated circular convolutions with and without normalization. We apply the powerful machinery of discrete Fourier transforms and circular convolutions to analyze the limiting behavior of the sequence of convolved and normalized polygons. This Fourier approach allows for a complete and insightful understanding of the limiting forms for a large class of polygons. In particular, we investigate generic, e.g. randomly generated planar polygons, as well as star-shaped polygons. In the case of random polygons, the key insight from

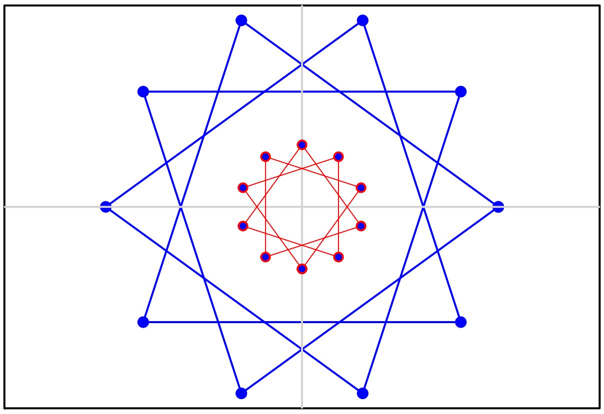

Fig. 9 A 3rd order, star-shaped 10-gon, after 5 normalized, circular convolutions.

this approach is the observation that the repeated application of circular convolution with normalization removes the higher harmonic pairs in the Fourier transform of the original polygon, and after sufficiently many convolutions, the scaled down principal harmonic pair dominates the Fourier transform of the repeatedly convolved and normalized polygon, thereby controlling the limiting elliptical shape. However, in the case of star-shaped polygons, the iterated, normalized circular convolutions result in a simple rotation and scaling of the original polygon, and the elliptical limiting behavior is not valid anymore.

In addition to planar polygons, we have been investigating the iterated normalized circular convolutions of higher dimensional, random polygons. We hope to complete and publish the higher-dimensional results soon. The problems we consider in this study have connections to a number of important mathematical tools and this opens up a rich area for investigations from a pedagogical perspective as well. The machinery being used includes circular convolutions, discrete Fourier transforms and their inverses, the Convolution theorem, Parseval's relation, a complex representation of an ellipse, and basic notions from linear algebra.

The mid-point averaging map is a linear transformaton that is closely related to the heat equation: the vertex coordinates of the new polygon are averages of the vertex coordinates of the original one. In that context, we recently discovered another potentially useful application of repeated polygon averaging to mathematical finance, more specifically, the pricing of financial derivatives, and we hope to complete and publish these results soon. There are various applications of polygon smoothing in the context of multiscale filtering of signals, including digital imaging and computer graphics. Polygon smoothing, with normalizations, appears in affine invariant evolution processes for smoothing planar curves, derived from an affine geometric heat flow. An interesting future project would be to investigate the limiting polygon forms resulting from iterated, normalized circular convolutions, using the *discrete, fractional Fourier transform.*

As one of the goals of this paper is to shed new light on this beautiful subject, we hope that it will attract the attention of students and researchers in engineering, physics and other applied fields.

Acknowledgements We thank the three referees, the associate editor and the editor-in-chief for their constructive criticism and suggestions for improving the paper.

References

1. Elmachtoub, A. N., Van Loan, C.F., From Random Polygon to Ellipse: An Eigenanalysis, SIAM Review, Vol. 52, No. 1, pp. 151–170 (2010). Permalink: http://dx.doi.org/10.1137/090746707.
2. Darboux, G., Sur un problème de géométrie élémentaire. Bull. Sci. Math. 2 (1878), 298-304. Stable url: http://www.numdam.org/item?id=BSMA_1878_2_2_1_298_1
3. Douglas, J., Geometry of polygons in the complex plane, Journal of Mathematics and Physics, Vol. 19, pp. 93–130 (1940).
4. Douglas, J., On linear polygon transformations, Bulletin of the American Mathematical Society, Vol. 46, Number 6, pp. 551–560 (1940).
5. Schoenberg, I.J., The finite Fourier series and elementary geometry, Amer. Math. Monthly 57 (1950), 390-404.
6. Cadwell, J.H., A property of linear cyclic transformations, Mathematical Gazette 37 (1953), 85-89.
7. Berlekamp, E.R., Gilbert, E.N. and Sinden, F.W., A polygon problem, Amer. Math. Monthly 72 (1965), 233-241.
8. Fejes Tóth, L., Iteration methods for convex polygons, Mat. Lapok 20 (1969), 15-23 (in Hungarian).
9. Fejes Tóth, L., Iteration processes leading to a regular polygon, Mat. Lapok 23 (1970), 135-141 (in Hungarian).
10. Davis, P.J., Cyclic transformations of polygons and the generalized inverse, Canadian J. Math. 39 (1977), 756-700.
11. Clarke, R.J., Sequences of Polygons, Math. Magazine, Vol. 52, No. 2, pp. 102–105 (1979).
12. Davis, P.J., Cyclic transformations of n-gons and related quadratic forms, Linear Algebra Appl. (1979) 25:57-75.
13. Davis, P.J., Circulant Matrices, Wiley, New York, 1979.
14. Chang, G., Davis, P.J., A circulant formulation of the Napoleon-Douglas-Neumann theorem, Linear Algebra Appl. 54 (1983), 87-95.
15. Chang, G., Davis, P.J., Iterative Processes in Elementary Geometry, Amer. Math. Monthly (1983), 90:7, 421-431.
16. Fisher, J.C., Ruoff, D., Shilleto, J., Perpendicular polygons. Amer. Math. Monthly 92, 2337 (1985).
17. Grünbaum, B., Lecture Notes on Modern Elementary Geometry. EPrint Collection, University of Washington (1999). Permalink: http://hdl.handle.net/1773/15592
18. Shapiro, D.B., A periodicity problem in plane geometry, Amer. Math. Monthly 99 (1984), 97-108.
19. Sapiro, G., Bruckstein, A., The ubiquitous ellipse, Acta Appl. Math. 38 (1995), 149-161.
20. Grégoire N., Convolution filters for polygons and the Petr-Douglas-Neumann theorem, Beitr Algebra Geom (2013) 54:701708.
21. Schwartz, R. E., The Projective Heat Map. AMS Monographs and Surveys Series (to appear).
22. Witkin, A.P., Scale-space filtering, Internat. Joint. Conf. Artificial Intelligence (1983), 1019-1021.
23. Shcherbakov, P.S., Formation control: The van Loan scheme and other algorithms, Automation and Remote Control (Springer 2011), 72:2210, doi: 10.1134/S0005117911100195.

24. Proskurnikov A.V., Parsegov, S.E., Problem of uniform deployment on a line segment for second-order agents, Automation and Remote Control (Springer 2016), 77:7, 1248-1258, doi: 10.1134/S0005117916070110.
25. The R Project for Statistical Computing. Stable url: `https://www.r-project.org`
26. Kostadinov, B., Simulation Insights Using R, PRIMUS: Problems, Resources, and Issues in Mathematics Undergraduate Studies, 23(3), pp. 208–223 (2013).
27. Montgomery, H.L., Early Fourier Analysis, pp. 33–51. AMS (2014).
28. Walker, J.S., Fast Fourier Transforms. CRC Press (1996).